STATUS OF ARSENIC CONTAMINATION IN THE GROUND WATER OF NAWALPARASI WEST DISTRICT AND REMEDIATION USING $ZnCl_2$ ACTIVATED SUGARCANE BAGASSE AS BIOADSORBENT

A RESEARCH FINAL REPORT SUBMITTED TO THE

TRIBHUVAN UNIVERSITY

INSTITUTE OF SCIENCE AND TECHNOLOGY(IoST)
DEAN'S OFFICE
KIRTIPUR, KATHMANDU, NEPAL
FOR THE MINI RESEARCH GRANT

By
Khag Raj Ghimire
Lecturer
Department of Chemistry
Butwal Multiple Campus
Tribhuvan Universty
Lumbini Province, Butwal, Nepal

Mentor: Dr. Bhoj Raj Poudel
Lecturer
Department of Chemistry
Tri-Chandra Multiple Campus
Tribhuvan University,Kathmandu

March,2024

1. INTRODUCTION

Arsenic comes in two forms: inorganic and organic. The most hazardous kind is thought to be inorganic (Velazquez-Jimenez et al., 2018). Inorganic As can be present as -3,0,+3,+5 oxidation states with arsenates (+5) in oxidizing environments and arsenites (+3) in mildly reducing conditions (Poudel et al., 2021). Groundwater is primarily contaminated by As from natural processes like weathering minerals, anthropogenic sources like poorly managed discharge from industries and As containing pesticides (Shakoor et al., 2019). Arsenic is very toxic in nature. Its negative effects are primarily induced by inactive enzymes in the cellular energy system, where arsenic combines with (-SH) groups of proteins and enzymes, limiting their catalytic function. In oxidizing environment arsenic sulfide converts into arsenic trioxide. Arsenic oxide dissolves easily in water and it has no taste, smell, or color. Hence it is challenging for the victim to realize that they are being poisoned. Since it is a cumulative poison, small doses taken over an extended length of time can lead to death (Parascandola, 2012).

Symptoms of acute arsenic poisoning, like vomiting, pain in abdomen, nausea, diarrhea, were often easily confused with those of other common illnesses. (Hughes et al., 2011). Chronic poisoning can result in keratosis, hyperkeratosis, cancer, heart problems, nerve damage, miscarriages, preterm birth etc. Thus, the WHO have set maximum acceptable limit of 10 µg/L (ppb) for arsenic (Velazquez-Jimenez et al., 2018). However, 50 ppb have been set by National Drinking Water Quality Standards, Nepal (NDWQS, 2006). Nearly 50% of Nepal's population are in Terai region and majority of them gets their drinking water from groundwater sources. However most of these sources are contaminated with bacteria and As. Several Terai districts in Nepal have been primarily affected by arsenic poisoning (Timalsina et al., 2021).

The threat of arsenic contamination of drinking water resources seems worldwide. Thus, it is urgently needed to remove arsenic from drinking water. Numerous approaches have been employed to remediate As from water. In terms of ease of use and cost of operation, adsorption process have been proven to be more effective than other approaches indicated above (Velazquez-Jimenez et al., 2018). Chemically modified biosorbents had greater adsorption capabilities than raw or unmodified biosorbent (Al-Rashdi et al., 2011).

There are various methods available, including ion exchange, reverse osmosis, membrane

processes, precipitation, crystallization, etc., for the removal of higher concentrations of arsenic. However, the removal of trace concentrations of arsenic is challenging. In real practice, the above-mentioned methods are expensive for developing countries like Nepal. This study will develop a new, cheap, effective, eco-friendly, and promising material to remedy this research gap. Previous research have explored the usage of biomass-based adsorbent to remove heavy metals, including arsenic from water. To the best of our knowledge, a novel method for removing arsenic from aqueous solutions will include $ZnCl_2$ activated sugarcane bagasse ($ZnCl_2$@SCB).

2. MATERIALS AND METHODS

2.1 Reagents:

All the Reagents utilized were of the analytical grade and were used without any further purification steps.

2.2. Preparation of Raw Sugarcane bagasse (RSCB)

The sugarcane baggasse was collected from Butwol, was rinsed with water multiple times and left to air dry. The dried bagasse was grinded in grinder and then sieved through <212-micron mesh to obtain uniform size. The biomass was again cleaned with DW until a clear solution was obtained. After which, it was dried for 24 hours at 65°C in a hot air oven. The dry powder was stored in a clean plastic bottle for further use as raw adsorbent (RSCB)).

2.3. Preparation of ZnCl2 activated sugarcane baggase

The RSCB was activated with the $ZnCl_2$ salt. Activation targets the development of pores on the surface of the biomass (Saka et al., 2020). 10 g of RSCB was added to 100 mL of $ZnCl_2$ (20 g). The solution was shaken in a mechanical shaker at 190 rpm for 24 hours. The solution was filtered out. The resultant wet product was repeatedly washed with DW by the decantation process till neutral. It was subsequently desiccated for 24 h at 60°C in a hot air oven. The final yield was labeled as $ZnCl_2$@SCB (Narayanan et al., 2023)

2.4. Characterization of Adsorbents

The phyico-chemical characterization of raw and ZnCl2 activated sugarcane baggasse was performed by FTIR, SEM, and XRD.

2.5. Influence of pH

The pH studies were done by shaking 20 mg of biosorbent in 20 mL of 20 mg/L of serial of As(V) solutions of pH 2.0 to 12.0 for 24 h. A mechanical shaker was used to agitate each

sample in a reagent bottle. The filtrate was utilized to analyse the residual As (V) concentration. The study compared final concentrations with initial concentrations to determine adsorptive removal percentages. The experiment was performed in triplicate, and mean value was calculated to ensure accuracy and reliability.

2.6. Influence of contact time

Kinetic tests were performed by adding 20 mg of adsorbents with 20 mL of an arsenite solution of 2o mg/L in the reagent bottles at optimum pH. The bottles were subjected to varying durations of shaking in a mechanical shaker, ranging from 10 to 300 minutes. After that, solutions were filtered at the respective time intervals. Furthermore, the level of As (V) before and after adsorption was analysed through a spectrophotometer.

2.7. Influence of initial concentration

Arsenite solutions variable from 5 to 400 mg/L were made. 25 mL of each solution were taken in clean, dry stopper bottles to achieve the optimum pH. 5 mL of each adjusted solution were then taken to measure the initial concentration using spectrophotometry. Every bottle was then filled with 20 mg of adsorbent. They were subjected to a 24-hour mechanical shaker set at 190 rpm. Following that, filtration was done, and the filtrate concentration was determined spectrophotometrically. The same data were used to conduct an isotherm study as well.

Collection of water sample and analysis of arsenic

Groundwater samples were taken in Ramgram, Nawalparasi West, Lumbini Province, Nepal, from an arsenic-contaminated location. Water samples were collected from 15 hand pumps which are below 20 feet in depth and from 5 samples from different surface water such as rivers, pond, water canal and from water deposite in field carefully in 50 ml glass bottle sealed with rubber cork. The details of the sampling and analysis protocols are described as follows. Prior to sampling, the hand pumps were flushed with 30–40 L of water. Water was filled into the bottle until it was completely full, with no air bubbles present. For the determination of total arsenic, samples were acidified with 2% v/v HCl. Following sampling, pH measurements were made immediately in the field.

The biosorption capability of $ZnCl_2$@SCB was examined using groundwater tainted with arsenic to determine the viability of $ZnCl_2$@SCB for removing arsenic from real sample of water.

3. RESULTS AND DISCUSSION

3.1. Characterization of Adsorbents

3.1.1. FTIR

Figure 1 displays the FTIR spectra of RSCB, $ZnCl_2$@SCB and As-$ZnCl_2$@SCB. The main functional group found in both Raw and activated bagasse is located at 3430 cm^{-1} and is associated with the hydroxyl group of OH. Since arsenic interacted with a component of the O-H structure, this band shifted to 3405 cm^{-1}, respectively (Sheng et al., 2014). Both raw RSCB and activated $ZnCl_2$@SCB exhibit the -CH_2 stretching band at 1370 cm^{-1}, suggesting that this functional group is responsible for the biosorption of arsenic. Consequently, two key observations are made: first, following activation and adsorption, most of the functional groups persisted in the material; second, following activation, the intensity of the functional groups significantly dropped.

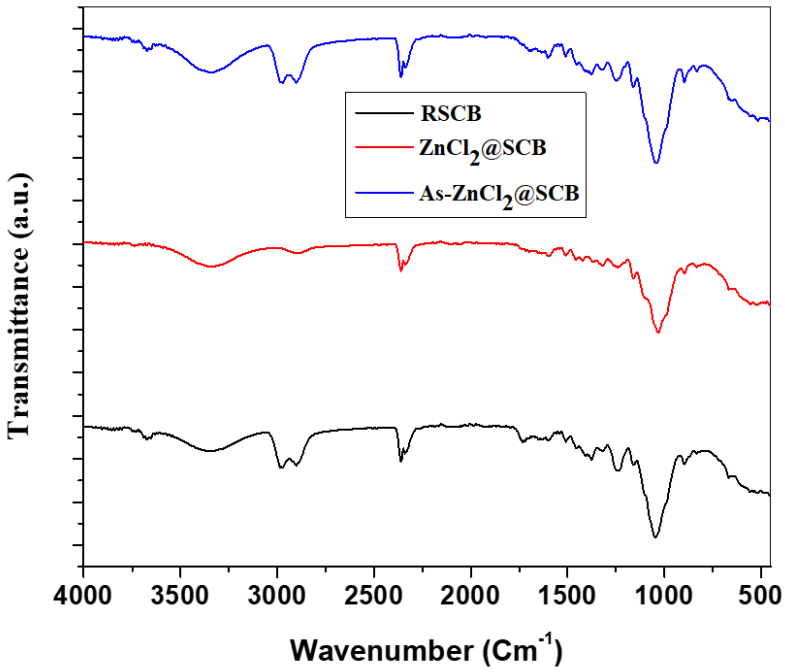

Figure 4.4 FTIR spectra of biosorbent

3.1.2. XRD

XRD patterns of RSCB and $ZnCl_2$@SCB before and after arsenic biosorption are displayed in **Figures 2**. The XRD pattern of RCB shows a prominent peak at 2θ value of 22.39º which corresponds to the typical characteristic peak positions of a crystalline form of cellulose. Some of the diffused and weak peaks represent the amorphous structure is predominant in the original biomass (Abdelhameed et al., 2020). According to this, RSCB is made up of both crystalline and amorphous structures. After activation, new broad peaks appeared. The emergence of new peaks in activated GB confirms the successful incorporation of $ZnCl_2$ into

RSCB. As-$ZnCl_2$@SCB retain the broad peak, indicating that only the amorphous area changes when activated biomass adsorbed As(V).

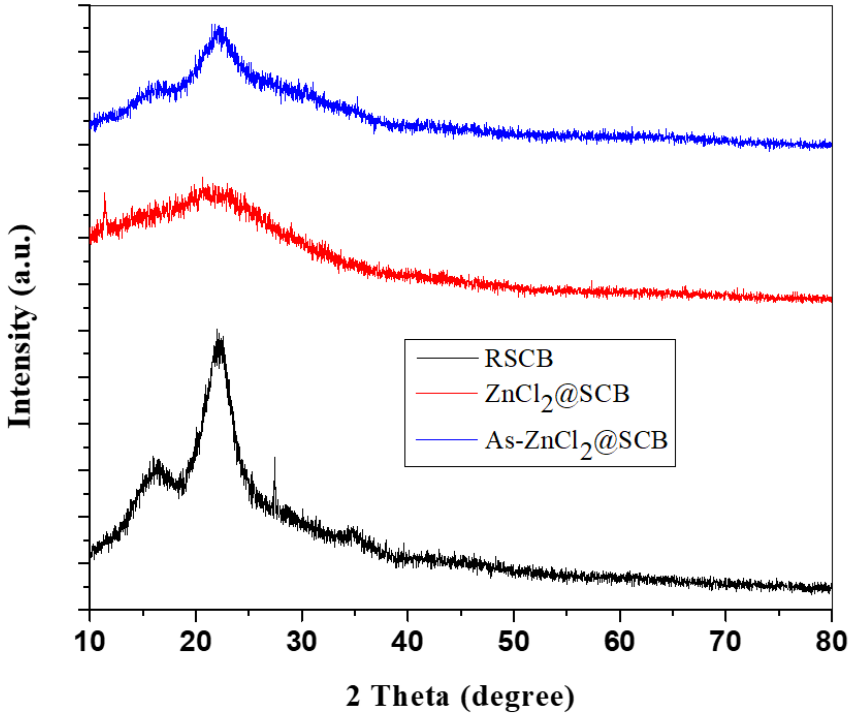

Figure 2: XRD pattern of RCB, $ZnCl_2$@SCB and As-$ZnCl_2$@RCB

3.2. Evaluation of λmax and Construction of Calibration Curve

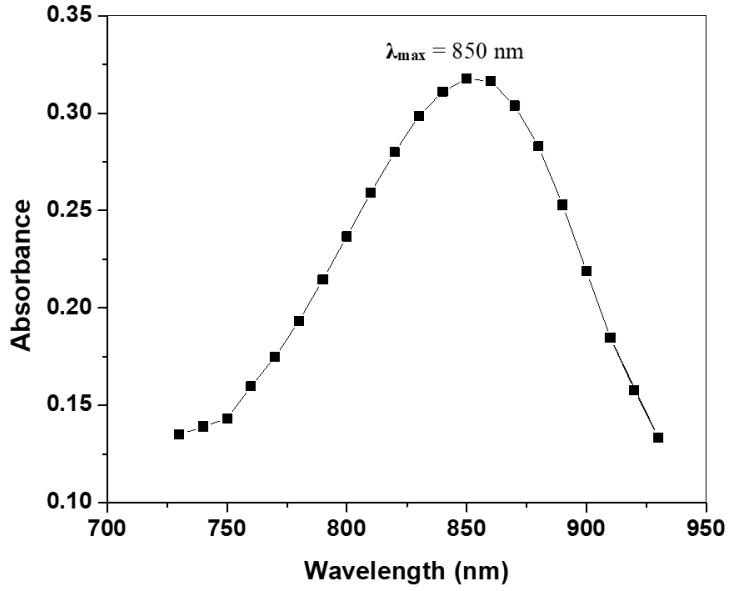

Figure 3: Absorbance plot for arsenomolybdenum blue complex

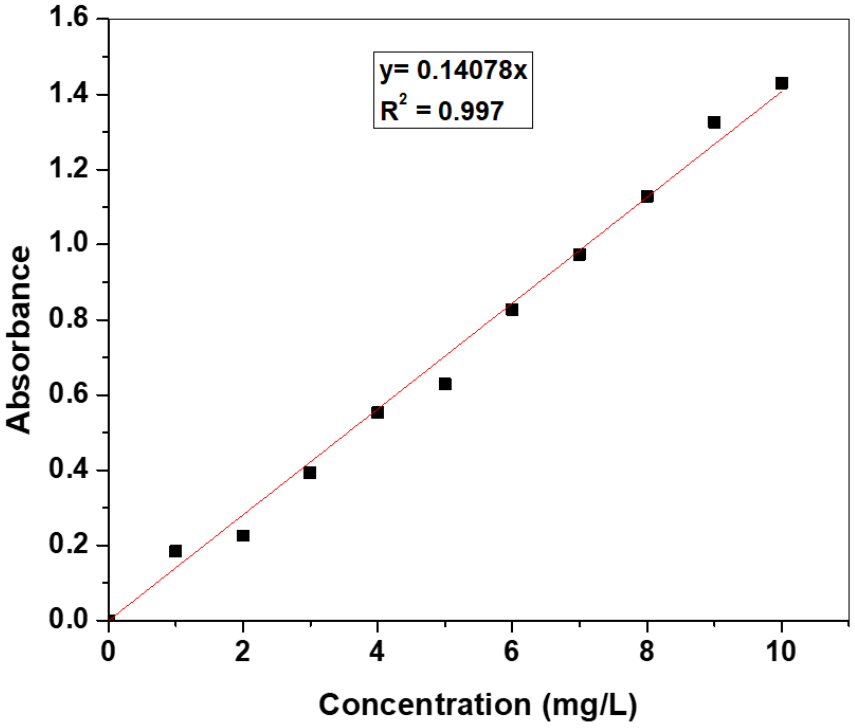

Figure 4: Absorbance *vs* concentration

A UV-Visible double beam spectrophotometer (Labtronics, LT-2802, India) was used to measure the concentration of As(V) in the test solution both before and after adsorption using a colorimetric method in the presence of ammonium molybdate and potassium antimonyl tartrate (λmax = 850 nm).

3.3. Influence of pH

The biosorption of ionic adsorbate is affected by the pH of solution because H^+ ions are powerful competitive ions. It affects the sorbent's functional group ionization as well as the sorbate's chemical composition in the solution. As (V) was absorbed using RSCB in a variety of pH ranges between 2 and 12, with no chemical modification. **Figure 5** indicates that As (V) adsorption by the raw biomass (RSCB) is negligible. Thus, it was not convenient to use RSCB as an arsenic removal agent. Therefore, $ZnCl_2$@SCB was used for subsequent testing and the findings were significantly better than those RSCB.

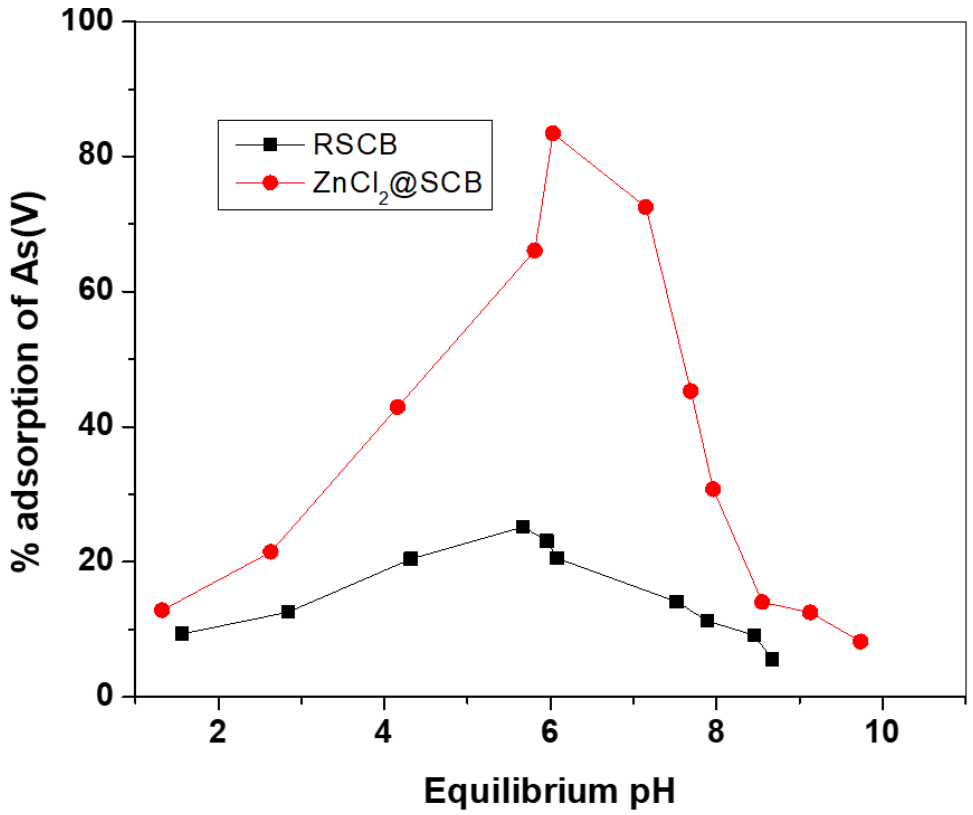

Figure 5: Variation of % adsorption with equilibrium pH of the solution

The arsenic removal percentage at various pH values is displayed using both RSCB and $ZnCl_2$@SCB. This study showed that raising the pH value from 3 to 7 a larger percentage of biosorption was seen, and at a pH higher than 7.0, the percentage of biosorption dramatically decreased. The greatest % adsorption efficiency was noted at pH 5.0. When the pH increased further, the adsorbent's sorption capacity diminished, as seen in **Figure 5.** Less than 15% of As(V) was removed from raw SCB. However, $ZnCl_2$@SCB displayed a remarkable As(V) removal percentage of up to 83.1%.

In a strongly acidic medium at pH < 2.3, As(V) mostly occurs as a neutral H_3AsO_4 species, and the biosorbent surfaces are exceedingly protonated, subsequently biosorption is unfavorable. Anionic species ($H_2AsO_4^-$ and $HAsO_4^{3-}$) can be formed when H_3AsO_4 deprotonates at pH values between 2.3 and 6.0. The +vely charged biosorbent surface attracts the negatively charged H_2AsO_4- and $HAsO_4^{2-}$. At a pH higher than 7.0 the percentage of biosorption dramatically decreased. Biosorption of As(V) anions may be significantly reduced at high pH > 7 due to competition for biosorption sites between OH^- ions and As(V) anions (Poudel et. al., 2021).

3.4. Influence of Contact Time

As the contact time increases, the biosorption significantly increases till it scopes the equilibrium point. Once the equilibrium time is reached, there is no considerable increase in adsorption rate because adsorption sites get almost full.

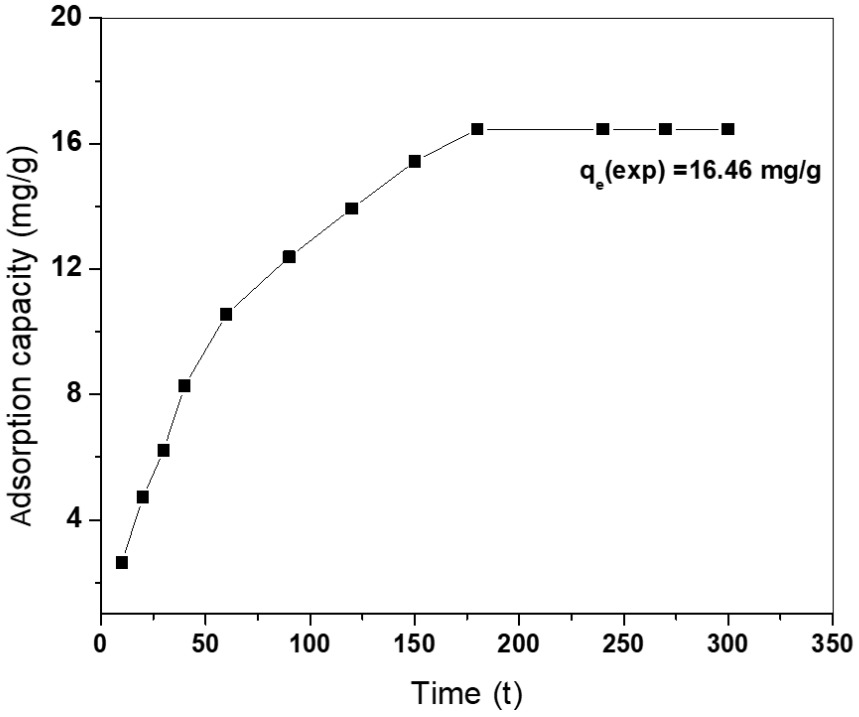

Figure 6: Variation of the As(V) uptake capacity onto $ZnCl_2$@SCB *vs* time.

Figure 6 displays the equilibrium contact time for As(V) removal on $ZnCl_2$@SCB is 3 hours. In the initial stages, the adsorption rate was higher because there were many active sites. The active sites are becoming more and more saturated with As (V) ions over a period of time. Following this, the adsorption rate gradually decreased until it attained adsorption equilibrium. Consequently, it is shown that the biosorption rate is directly related to the number of accessible adsorption sites. Even though equilibrium was reached in 3 hours, further work was done for 10 hours to make sure the equilibrium was completely reached.

3.5. Kinetic Modeling

The experiment was analyzed using pseudo firs-order (PFO) and pseudo-second order (PSO) kinetic models to identify the top fitting kinetic model and evaluate the adsorption mechanism. The plot of "log(qe-qt)" vs "time" is displayed by the PFO model (**Figure 7**), and the plot of "t/qt" versus "time" is displayed by the PSO model (**Figure 8**).

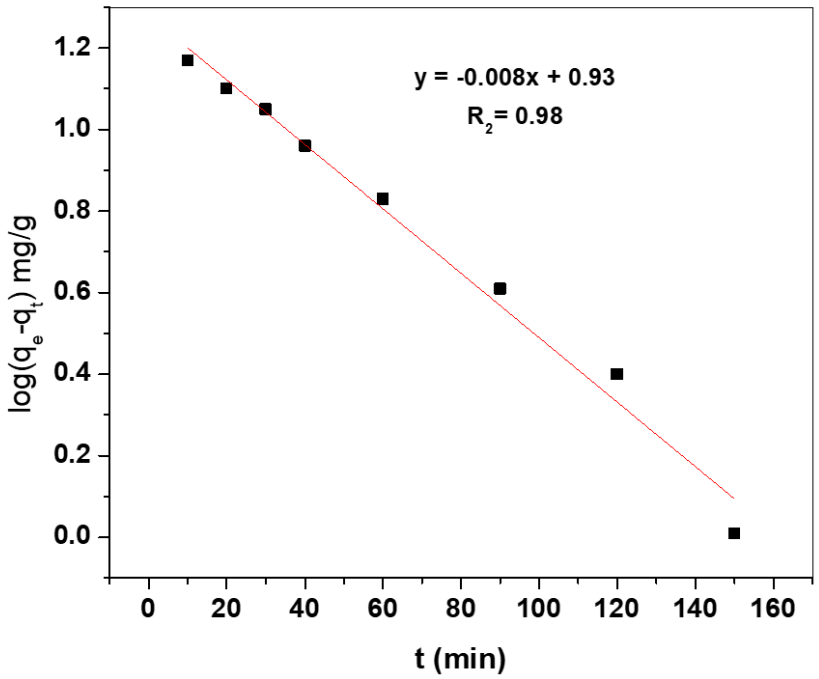

Figure 7: PFO kinetic plot

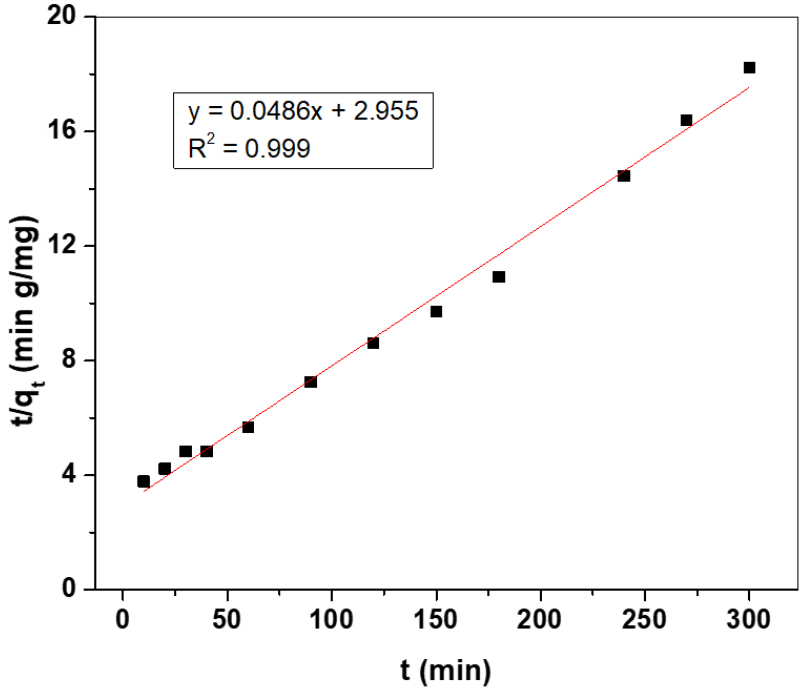

Figure 8: PSO kinetic plot

The plots of PFO and PSO models, generated the straight lines. However PSO kinetics has a higher R^2 value than PFO kinetics.

Table 1: Kinetic parameters for As(V) biosorption on $ZnCl_2$@SCB

Model	R^2	q_e (exp) (mg/g)	q_e (cal) (mg/g)	k_1 (min^{-1})	k_2 (g /mg.min)
PSO	0.999	16.46	16.94	-	1.17×10^{-3}
PFO	0.980	16.46	8.51	0.010	-

Based on the qe value, the kinetic modeling of every adsorption was explained in the above table. When the qe values of both orders were compared, the PSO value agreed more closely with the experimentally determined qe value (16.46 mg/g). According to the PSO model, the As(V) uptake capacity is 16.94 mg/g, whereas the PFO model yields 8.51 mg/g. Therefore, it can be resolved that the kinetic behavior of the biosorption is better predicted by PSO and chemisorptions is the rate-determining step (Agrafioti et al., 2014).

3.6. Influence of Concentration of As(V) Solution

It demonstrates that adsorption increases with increasing initial concentration of As(V) and reaches equilibrium since there are limited sorption sites available. It indicates that the biosorption trails the Langmuir isotherm. As arsenic concentration increases the mass transfer driving forces are enhanced. It accelerates the movement of As(V) anions from bulk solution to the surface of biosorbent and leads to increased adsorption. After equilibrium, there is a gradual decrease in percentage removal due to the decline in the adsorptive surface and ions competition for available binding sites on the adsorbent.

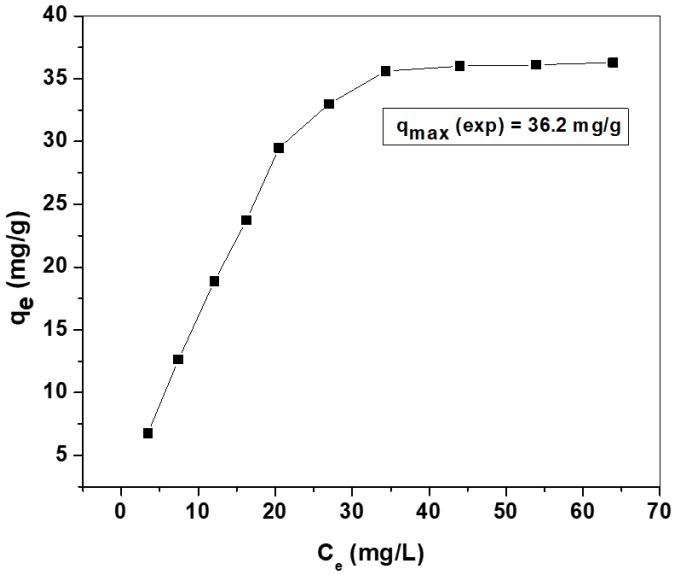

Figure 9: Variation of adsorption capacity of $ZnCl_2$@SCB with equilibrium concentration

3.8 Isotherm Modeling

The freundlich isotherm was plotted using 'logqe' vs. 'logCe' (**Figure 10**) and the Langmuir isotherm using data of 'Ce/qe' vs. 'Ce' (**Figure 11**). The Langmuir model was considered as the better suited model due to its high correlation coefficients. **Table 2** contains the evaluation results for the isotherm parameters. The Langmuir equilibrium parameter (K_L) was found to be 0.54 L/mg, while the Freundlich model's 1/n value was 0.67, which indicates the adsorption process is favorable. A Langmuir model was utilized to determine q_{max} of As(V) onto $ZnCl_2$@SCB which is 37.03 mg/g. This q_{max} value closely matches the 36.2 mg/g adsorption capacity found in the plateau region of the isotherm curve.

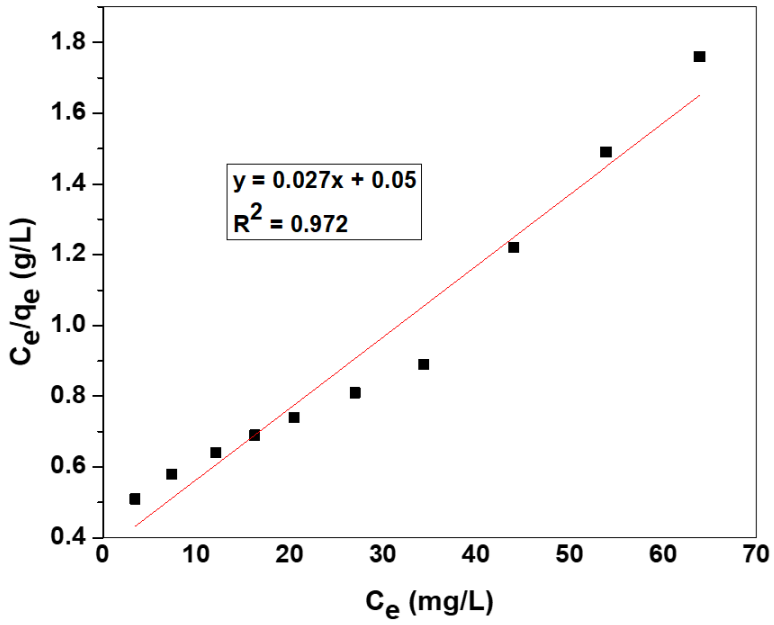

Figure 10: Langmuir adsorption isotherm plot

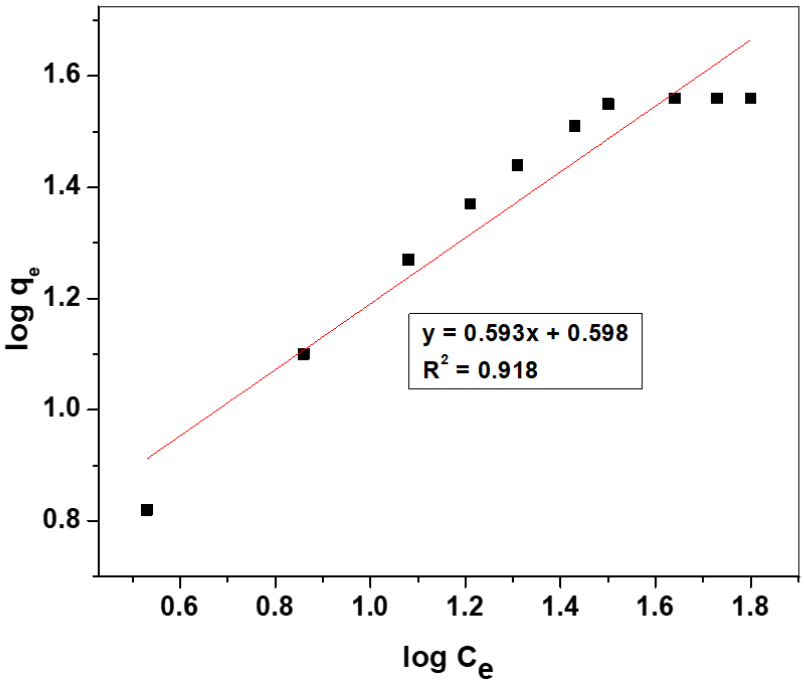

Figure 11: Freundlich adsorption isotherm plot

Table 2: Isotherm parameters for adsorption of As(V) onto $ZnCl_2$@SCB

Isotherm model	Parameter	Value
Langmuir isotherm	q_m(mg/mg)	37.03
	K_L (L/mg)	0.54
	R^2	0.972
Freundlich isotherm	K_F (mg/g) $(L/mg)^{1/n}$	3.96
	1/n	0.593
	R^2	0.918

4.8 Application of SPP@Zr to natural water

The collected 15 groundwater samples (g1 to G15) and 5 surface water samples (S1 to S5) were analysed for total arsenic concentrations by using AAS, and the findings are shown in **Figure 12**. It displays that arsenic content of six grounwater samples were found to be higher than the mark of drinking water tolerance threshold established by NDWQS (50 µg/L) and all ground water samples and two surface water samples were found to be higher than the mark

of drinking water tolerance threshold established by WHO (10 µg/L).

Batch biosorption tests using biosorbent doses 2 g/L were performed on water samples having high arsenic content at their native pH. The residual total arsenic concentrations were examined. It displays that arsenic content was found to be much lower than the mark of drinking water tolerance threshold established by WHO (10 µg/L), These results support the idea that $ZnCl_2$@SCB offers a possible method for removing arsenic from polluted water.

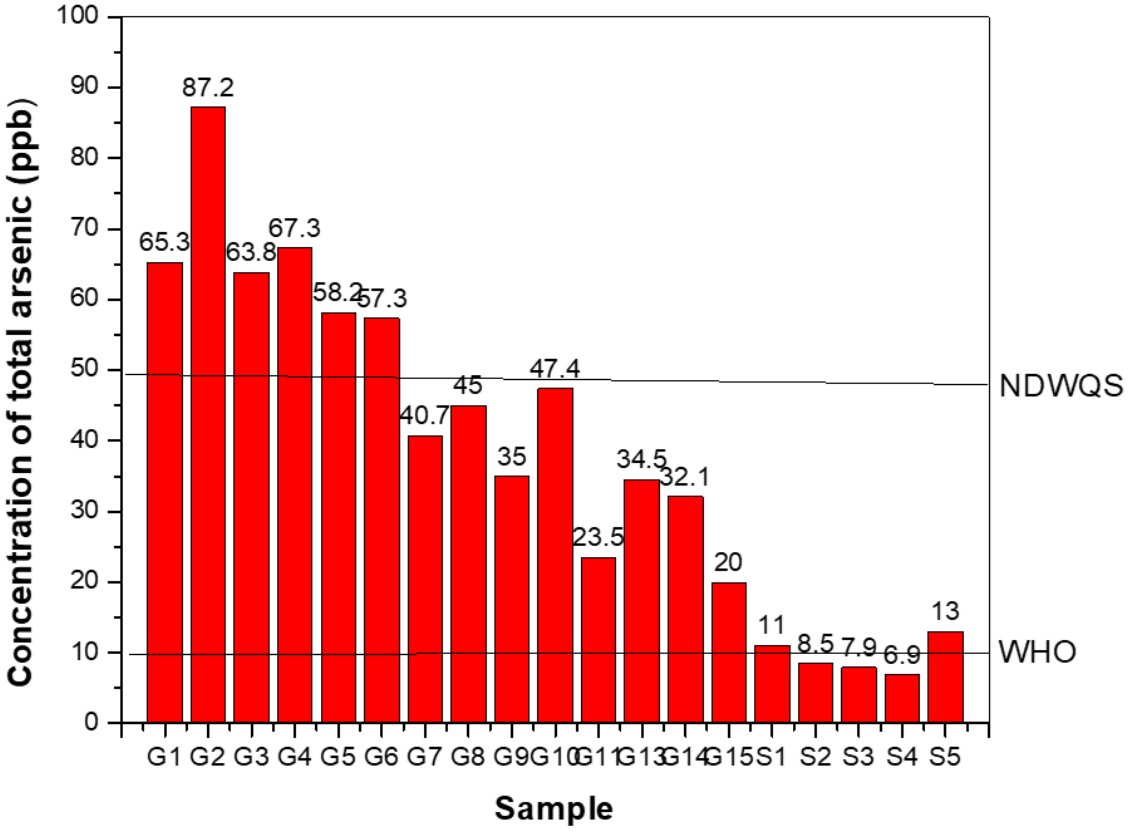

Figure 11: Total arsenic in groundwater samples (G1 to G15) and surface water samples (S1 to S5) collected from Ramgram, Nawalparasi west

REFERENCES

Abdelhameed, R. M., Alzahrani, E., Shaltout, A. A., & Moghazy, R. M. (2020). Development of biological macroalgae lignins using copper-based metal-organic framework for selective adsorption of cationic dye from mixed dyes. *International*

Journal of Biological Macromolecules, *165*, 2984-2993.

Agrafioti, E., Kalderis, D., &Diamadopoulos, E. (2014). Arsenic and chromium removal from water using biochars derived from rice husk, organic solid wastes and sewage sludge. *Journal of environmental management*, *133*, 309-314.

Al-Rashdi, B., Somerfield, C., &Hilal, N. (2011). Heavy Metals Removal Using Adsorption and Nanofiltration Techniques. *Separation & Purification Reviews*, *40*(3), Article 3. https://doi.org/10.1080/15422119.2011.558165.

Hughes, M. F., Beck, B. D., Chen, Y., Lewis, A. S., & Thomas, D. J. (2011). Arsenic Exposure and Toxicology: A Historical Perspective. *Toxicological Sciences*, *123*(2), Article 2. https://doi.org/10.1093/toxsci/kfr184.

Mittal, A., Mittal, J., Malviya, A., Kaur, D., & Gupta, V. K. (2010). Adsorption of hazardous dye crystal violet from wastewater by waste materials. *Journal of colloid and interface science*, *343*(2), 463-473.

Narayanan, I., Kumar, P. S., Franco, D. S., Georgin, J., Meili, L., & Selvasembian, R. (2023). Insight into the biosorptive removal mechanisms of hexavalent chromium using the red macroalgae Gelidium sp. *Biomass Conversion and Biorefinery*, 1-15.

National Drinking Water Quality Standards (NDWQS) 2062. (2006) Government of Nepal, Ministry of Physical Planning and Works, Kathmandu.

Parascandola, J. (2012). *King of poisons: a history of arsenic*. Potomac Books, Inc.

Saka, C., Kaya, M., & Bekiroğullari, M. (2020). Chlorella vulgaris microalgae strain modified with zinc chloride as a new support material for hydrogen production from NaBH4 methanolysis using CuB, NiB, and FeB metal catalysts. *International journal of hydrogen energy*, *45*(3), 1959-1968.

Shakoor, M. B., Niazi, N. K., Bibi, I., Shahid, M., Saqib, Z. A., Nawaz, M. F., ...&Rinklebe, J. (2019). Exploring the arsenic removal potential of various biosorbents from water. *Environment international*, *123*, 567-579.

Sheng, T., Baig, S. A., Hu, Y., Xue, X., &Xu, X. (2014). Development, characterization and evaluation of iron-coated honeycomb briquette cinders for the removal of As (V) from aqueous solutions. *Arabian Journal of Chemistry*, *7*(1), 27-36.

Timalsina, H., Mainali, B., Angove, M. J., Komai, T., & Paudel, S. R. (2021). Potential modification of groundwater arsenic removal filter commonly used in Nepal: A review. *Groundwater for Sustainable Development, 12*, 100549.

Velazquez-Jimenez, L. H., Arcibar-Orozco, J. A., & Rangel-Mendez, J. R. (2018). Overview of As (V) adsorption on Zr-functionalized activated carbon for aqueous streams remediation. *Journal of Environmental Management, 212*, 121–130.